Journal of Materials Chemistry C

Accepted Manuscript

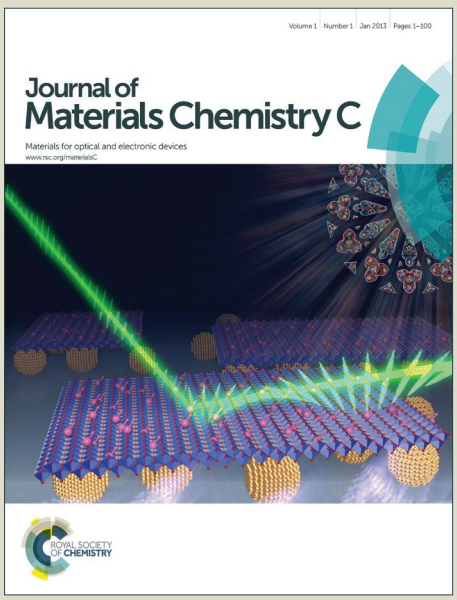

ROYAL SOCIETY OF CHEMISTRY

www.rsc.org/materialsC

Journal Name

ARTICLE

Enhanced lifetime of organic light-emitting diodes using soluble tetraalkyl-substituted copper phthalocyanines as anode buffer layers†

Received 00th January 20xx,
Accepted 00th January 20xx

DOI: 10.1039/x0xx00000x

www.rsc.org/

Jiaju Xu,‡[a] Yulong Wang,‡[a] Qian Chen,[a] Yiwei Lin,[a] Haiquan Shan,[a] V. A. L. Roy*[b] and Zongxiang Xu*[a]

This study describes two soluble tetraalkyl-substituted copper phthalocyanines (CuPcs) as hole-blocking materials that can be used in the Alq_3-based organic light-emitting diodes (OLEDs). The hole-blocking characteristics of these Pc layers significantly impeded hole injection into the Alq_3 emitting layer and thus decreased the production of unstable cationic Alq_3 species, giving the enhanced OLED efficiency and stability compared with that of devices containing the widely used PEDOT:PSS. Moreover, the insolubility of the CuPcs in water together with their extremely high thermal and chemical stability led to the effective protection of the ITO anode, resulting in the increased operational stability of the OLEDs in air and the enhancement of OLED durability.

Introduction

Hole injection layers (HILs) and hole transport layers (HTLs) are considered crucial for optimizing the performance of organic light-emitting diodes (OLEDs) because of the low intrinsic carrier concentration of organic semiconductors.[1-3] Because of its transparency in the visible spectral region, indium tin oxide (ITO) is the preferred anode material for optoelectronic devices. However, the relatively low work function of ITO anodes (4.7 eV), as well as the interface dipole at typical ITO/organic interfaces, usually cause large barriers for hole injection.[3] A popular strategy to promote hole injection in OLEDs is to insert a buffer layer between the ITO anode and emissive layer to facilitate effective hole migration from the anode to the emissive zone.[1,2,4-6] Poly(3,4-ethylenedioxythiophene):poly(styrene sulfonate) (PEDOT:PSS) is a widely used HIL/HTL because of its appropriate energy level for hole injection and transport together with its ability to form planar films, which lead to substantial improvements of luminous efficiency, brightness, external quantum efficiency, and device lifetime.[5,7-10] Also, spin-coated PEDOT:PSS thin films are insoluble in common organic solvents, which is essential to allow solution processing of electronic devices in multi-layered structures like polymer light-emitting diodes and organic photovoltaic solar cells.[2,11] However, a number of challenges such as exciton quenching, weak interface adhesion, degradation of neighboring organic layer, and corrosion of ITO electrodes still limit long-term device stability.[12-15] In particular, strongly acidic PSS (typical pH of 1.2[16]) is known to etch ITO during the PEDOT:PSS spin-coating process.[3,17] The hydrolysis of deposited PEDOT:PSS upon moisture exposure can also etch ITO and lead to the diffusion of indium into the active layer of the device.[13] Incorporation of indium has raised concerns about OLED durability and reliability.[3,18]

One current alternative to stabilize OLEDs relies on the replacement of PEDOT:PSS with other HIL materials such as metal phthalocyanines (Pcs)[19-25] and transition metal oxides like WO_3,[26] MoO_3,[27-31] and V_2O_5.[32] Among these materials, copper phthalocyanine (CuPc) is a popular choice for OLED anode buffer layers. Taking advantage of the appropriate highest occupied molecular orbital (HOMO) energy levels, extremely high thermal and chemical stabilities, favorable field-effect properties and non-toxicity of Pcs,[33-36] enhanced hole injection and improved device performance have been achieved by using CuPc as an anode buffer layer in OLEDs.[21] However, CuPc can induce crystallization of HTL N,N'-bis-(1-naphthalenyl)-N,N'-bis-phenyl-(1,1'-biphenyl)-4,4'-diamine (NPB), thus affecting the long-term stability of OLEDs containing both CuPc and NPB.[27] Moreover, the poor solubility of CuPc in common solvents means that buffer layer preparation involves vacuum sublimation, which potentially increases industrial production cost compared with that of solution processing.[37]

In this study, we report two soluble tetraalkyl-substituted CuPcs, **CuEtPc** and **CuBuPc** (Fig. 1a), as anode buffer layers to modify the ITO/HTL interface in OLEDs. The performance and durability of OLEDs containing **CuEtPc** and **CuBuPc** as anode buffer layers is assessed.

[a] Department of Chemistry, South University of Science and Technology of China, Shenzhen, P. R. China. Email: xuzx@sustc.edu.cn.
[b] Department of Physics and Materials Science, City University of Hong Kong, Hong Kong SAR. Email: val.roy@cityu.edu.hk.

† Footnotes relating to the title and/or authors should appear here.
Electronic Supplementary Information (ESI) available: [details of any supplementary information available should be included here]. See DOI: 10.1039/x0xx00000x
‡ These authors contributed equally.

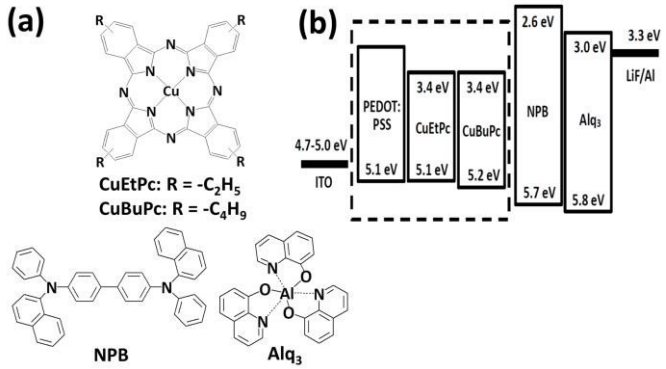

Fig. 1 (a) Chemical structures of the materials, and (b) Device configurations and energy level diagrams of the OLEDs in this work.

Table 1 Device structures of OLEDs

Device	Structure
Type I	ITO/NPB (50 nm)/Alq_3 (50 nm)/LiF (0.5 nm)/Al (100 nm)
Type II	ITO/PEDOT:PSS (48 nm)/NPB (50 nm)/Alq_3 (50 nm)/LiF (0.5 nm)/Al (100 nm)
Type III	ITO/CuEtPc (28 nm)/Alq_3 (50 nm)/LiF (0.5 nm)/Al (100 nm)
Type IV	ITO/CuBuPc (27 nm)/Alq_3 (50 nm)/LiF (0.5 nm)/Al (100 nm)

Experimental

Device fabrication and characterization

Four types of diodes were fabricated in this work; the device structures and energy level diagrams are illustrated in Table 1 and Fig. 1b, respectively. The influence of **CuEtPc** and **CuBuPc** anode buffer layers on device performance was compared with that of PEDOT:PSS and NPB. To understand the hole injection characteristics of the devices, a single HTL device (type I), was fabricated. To compare the device with alternative anode modifying layers, diode type II was fabricated using PEDOT:PSS as the anode buffer layer. The OLEDs were fabricated on patterned ITO glass with a sheet resistance of 20 Ω/□. The PEDOT:PSS buffer layer (Al 4083) was spin coated on the ITO surface at a rate of 4000 rpm, while the **CuEtPc** and **CuBuPc** layers were spin coated at a rate of 1000 rpm with 10 mg/mL solution in dichlorobenzene. The thickness of spin-coated layers was measured on a KLA-TENCOR D-100 profiler, and estimated to be 28, 27 and 48 nm for **CuEtPc**, **CuBuPc** and PEDOT:PSS, respectively. Other layers were deposited by thermal evaporation under a vacuum of ~1×10^{-6} Torr (Mbraun MB200). Layer thickness was monitored *in situ* using a quartz crystal monitor during deposition. After fabrication, all OLEDs were encapsulated using UV adhesive under a nitrogen atmosphere. The emissive area of the devices was 10 mm^2.

The current–voltage–luminance characteristics of the devices were recorded using an automatic system containing a source-measure unit (Keithley 2400) and calibrated spectrometer (Photo Research PR680). The surface morphologies of the ITO, PEDOT:PSS-modified ITO, and **CuEtPc**(**CuBuPc**)-modified ITO surfaces were examined using atomic force microscopy (AFM; VEECO Multimode V, tapping mode). All measurements were carried out under ambient conditions after device fabrication and encapsulation.

Materials

CuBuPc was synthesized according to a reported method,[38] and **CuEtPc** was prepared by a similar procedure (see Supplementary Information, ESI†). The Pc materials were further purified *via* vacuum sublimation to fulfill the purity requirements of electronics applications. The TGA measurements were performed, and both Pc materials exhibited an excellent thermal stability with a decomposition onset higher than 450 ℃ (Fig. S1, ESI†). All other materials were purchased from Sigma-Aldrich and used directly without further purification. The energy levels of the Pc materials were extracted from cyclic voltammetry data combined with UV-Vis absorption spectra according to a method described in the literature.[39] The HOMO levels of **CuEtPc** and **CuBuPc** were estimated to be 5.1 and 5.2 eV, respectively (Fig. 1b), making them suitable candidates as hole injection materials in OLEDs. The HOMO levels of ITO and NPB are 4.7–5.0 and 5.7 eV, respectively.[40]

Results and discussion

AFM analysis

Prior to device fabrication, the morphology of the ITO glass as well as the spin-coated PEDOT:PSS, **CuEtPc** and **CuBuPc** thin films on ITO glass substrates was characterized *via* AFM. The pristine ITO glass had a rough surface with a surface root-mean-square (RMS) roughness of 2.23 nm (Fig. 2a). Lower average surface RMS roughness values of 1.38 and 0.92 nm were determined for the **CuEtPc** and **CuBuPc** layers, respectively (Fig. 2c, d). **CuEtPc** and **CuBuPc** formed flat uniform films with comparable morphology to that of PEDOT:PSS, which had a surface RMS roughness of 1.28 nm, as illustrated in Fig. 2b.

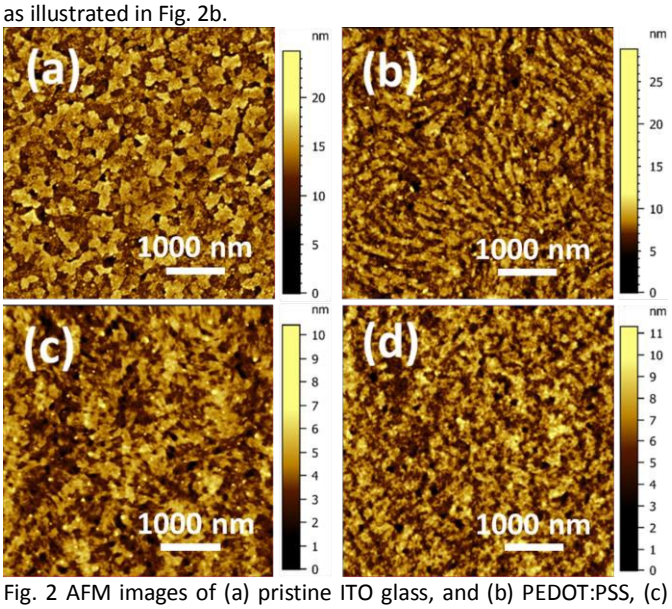

Fig. 2 AFM images of (a) pristine ITO glass, and (b) PEDOT:PSS, (c) **CuEtPc**, and (d) **CuBuPc** thin films spin-coated on ITO glass substrates.

OLED performances

Electroluminescence (EL) spectra of the four as-fabricated diodes are depicted in Fig. 3. All devices displayed emission maxima around 530 nm, consistent with the EL characteristics of Alq_3-based

OLED. These results show that these buffer layers do not substantially alter the emission spectrum of Alq_3. The performance of the diodes is summarized in Table 2.

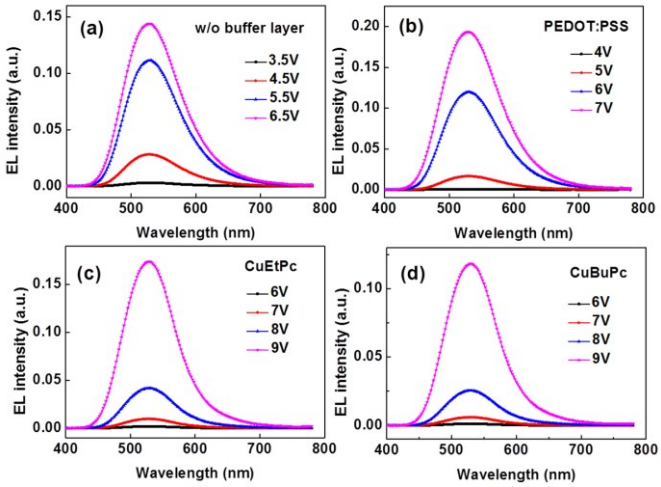

Fig. 3 Electroluminescence spectra of OLEDs at various operating voltages.

Table 2 Performance of OLEDs

Anodic buffer layer	$\lambda_{EL,max}$ [a] (nm)	CIE [b] (x, y)	$V_{turn-on}$ [c] (V)	LE_{max} [d] (cd/A)	PE_{max} [e] (lm/W)	L_{max} [f] (cd/m^2)
w/o buffer layer	530	0.313, 0.541	2.5	2.96	2.04	6966
PEDOT:PSS	530	0.314, 0.533	3.0	3.77	1.97	9477
CuEtPc	530	0.285, 0.547	4.0	3.24	1.36	9611
CuBuPc	530	0.292, 0.546	4.1	3.26	1.18	8213

[a] Maximum peak of EL spectra. [b] Measured at maximum luminance. [c] Turn-on voltage recorded at a luminance of 1 cd/m^2. [d] Maximum luminous efficiency. [e] Maximum power efficiency. [f] Maximum luminance

The luminance–voltage (L-V) characteristics of the diodes are presented in Fig. 4a. Inserting a buffer layer (PEDOT:PSS, **CuEtPc** or **CuBuPc**) causes the L-V characteristics to shift to higher voltage. Turn-on voltages of 3.0, 4.0 and 4.1 V were found for OLEDs containing PEDOT:PSS, **CuEtPc** and **CuBuPc**, respectively, while that of the single HTL diode (type I) was only 2.5 V (Table 2). This indicates that these anode buffer layers impede hole injection into the HTL.[41] The significant property of hole-blocking of the Pc layers compared to that of PEDOT:PSS (also evidenced by the characterization of hole-only devices, Fig. S2, ESI†) is possibly due to the alkyl groups of the Pc structures that formed a thin "insulating layers" at both ITO/**CuEtPc**(**CuBuPc**) and **CuEtPc**(**CuBuPc**)/NPB interfaces. The luminance of the OLEDs was improved by inclusion of a buffer layer between the ITO anode and NPB layer. The OLEDs with **CuEtPc** and **CuBuPc** exhibited comparable EL characteristics to that of the diode containing PEDOT:PSS. The highest maximum brightness of 9611 cd/m^2 was observed for the OLED with **CuEtPc** (Table 2). For Alq_3-based OLEDs, hole injection into Alq_3 leads to a decrease in its fluorescence quantum yield due to the degradation products of the unstable cationic Alq_3 species that acted as fluorescence quenchers.[41] Thus, the increased brightness of the OLED with **CuEtPc** can be attributed to this buffer layer slowing down the hole injection into the Alq_3 emissive layer.

The improvement of charge balance achieved by inserting a **CuEtPc** or **CuBuPc** layer between the ITO anode and HTL in the OLEDs can also be observed in their luminance–current density (L-J) curves, as shown in Fig. 4b. The luminance of all diodes increases linearly with current density at relatively low current density (0–100 mA/cm^2). However, when the current density exceeds 100 mA/cm^2, a roll-off effect is observed in the L-J curve of the diode without an anode buffer layer. This indicates poor charge balance in this device compared with that in the other ones. Possible reasons for the poor charge balance include exciton–exciton interactions, exciton–charge carrier interactions, and exciton dissociation at high current density.[42-44] Another possible cause is the blocking of hole migration into the NPB/Alq_3 interface by these buffer layers.[41] At higher current density, electron density in the Alq_3 layer neighboring to NPB/Alq_3 interface is increased. The high electron density at the NPB/Alq_3 interface greatly lowers the production of cationic Alq_3 species, resulting in direct hole injection into anionic Alq_3 species from NPB to generate excited states.[41,45] It should be noted that the OLEDs with **CuEtPc** and **CuBuPc** exhibit superior L-J behavior relative to that of the diode containing PEDOT:PSS. As shown in Fig. 4b, a more pronounced roll-off effect is observed for the diode with PEDOT:PSS than those with **CuEtPc** and **CuBuPc** at higher current density, demonstrating the improved charge balance and optimization of charge carrier flow into the Alq_3 layer upon inserting a Pc buffer layer in the OLEDs.

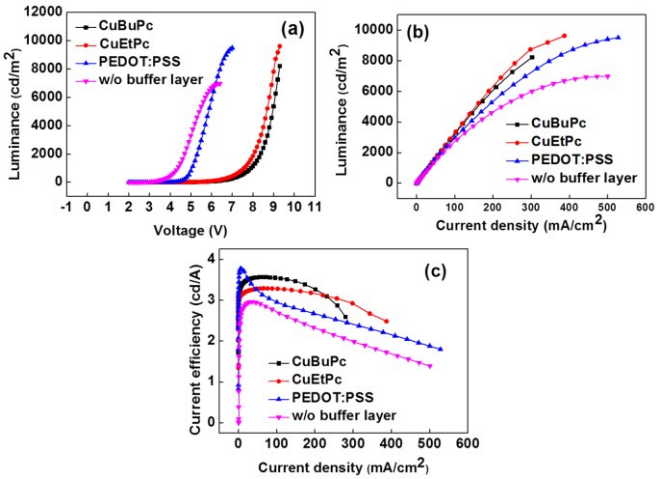

Fig. 4 (a) Luminance–voltage, and (b) Luminance–current density characteristics of OLEDs. (c) Current efficiency as a function of current density of OLEDs.

Among the three types of ITO-modified diodes, superior EL efficiencies are observed for the ones with **CuEtPc** and **CuBuPc** buffer layers compared with that containing PEDOT:PSS. As illustrated in Fig. 4c, although the highest maximum efficiency of 3.77 cd/A is obtained for the OLED with PEDOT:PSS at a low current density of 6.5 mA/cm^2, the diodes with **CuEtPc** and **CuBuPc** generally exhibit higher EL efficiency than that of the OLED with PEDOT:PSS over the main measurement range. Fig. 4a reveals that considerable positive shifts in L-V characteristics are observed for

the diodes with **CuEtPc** and **CuBuPc** compared with that of PEDOT:PSS (*i.e.*, **CuBuPc** > **CuEtPc** > PEDOT:PSS). This suggests that there is increased hole impedance into NPB by these Pc layers compared with that in the case of PEDOT:PSS. The increased hole impedance into NPB and Alq_3 by the Pc hole-blocking layers led to lower hole/electron ratios at the NPB/Alq_3 interface and thus achieved more balanced electron and hole injection processes, resulting in improved EL efficiencies.[41,45,46]

OLED lifetime studies

To investigate the effect of the Pc buffer layer quality as well as the enhancement of charge balance of OLEDs on device stability, the long-term degradation performance of OLEDs was examined. The stability measurements were performed under a constant driving current density of 100 mA/cm^2, at which roughly the same initial brightness (~3000 cd/m^2) was obtained for each diode. In addition to the efficiency enhancement, the operating lifetime was also improved markedly by the Pc buffer layers, as shown in Fig. 5a. The luminance of the device without a buffer layer decayed rapidly, exhibiting a poor half-life time of 355 min. The OLED lifetime was increased by inserting a PEDOT:PSS layer, giving an improved half-lifetime of 619 min. Substantial improvement of device durability was obtained for OLEDs containing Pc layers compared with those of the single HTL device and the with PEDOT:PSS; namely, half-lifetimes as long as 1783 and 2171 min were observed for diodes with **CuEtPc** and **CuBuPc** buffer layers, respectively. The device stability is also reflected by the voltage stability. Fig. 5b presents the operating voltage as a function of time for OLEDs with and without buffer layers. The diodes with **CuEtPc** and **CuBuPc** buffer layers exhibited very stable operating voltages over the whole operating period compared with those of the other two devices. For instance, after 1200 min of operation, voltage rises of ~113% and ~20% were found for the devices with a single HTL and PEDOT:PSS, respectively, while a voltage rise of only ~5% was measured for the OLEDs with **CuEtPc** and **CuBuPc** layers.

OLED degradation was further studied by observation of dark spot growth of the diodes during device operation. Fig. 6 illustrates a series of micrographs of the OLEDs taken after 20, 40, 60, 80, 100 and 120 h of operation under ambient conditions. The OLED without a buffer layer shows a remarkable increase in dark spot growth compared with those of the modified ITO diodes, revealing the role of these anode buffer layers in retarding the growth of dark spots. Although all the micrographs display an increase in the area of the dark spots over time, the dark spot growth in the OLED with **CuBuPc** was much lower compared with that in the other three diodes. Also, dark spot growth in the OLED with PEDOT:PSS was more extensive than that in the case of the OLED containing **CuEtPc**. These results are consistent with the lifetime measurements for the diodes.

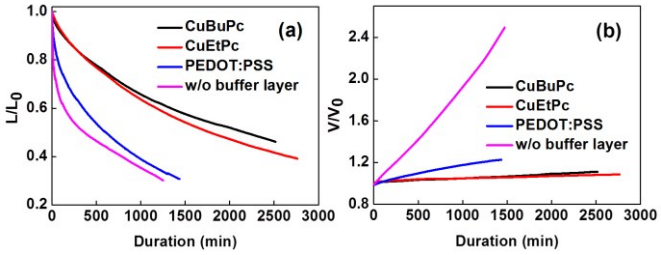

Fig. 5 (a) Normalized luminance, and (b) Normalized operating voltage versus time of the OLEDs under a constant current density of 100 mA/cm^2.

Clearly, there is a strong correlation between hole injection/transport into Alq_3 and the device lifetime of the Alq_3-based OLEDs.[41] In fact, the decrease in hole injection or transport induced by the Pc buffer layers led to longer operating lifetime because the recombination zone moved away from the cathode.[17,41] Under these conditions, the increased the electron density at the HTL/Alq_3 interface greatly decreased the production of unstable cationic Alq_3 species, which led to the enhanced device stability.[41]

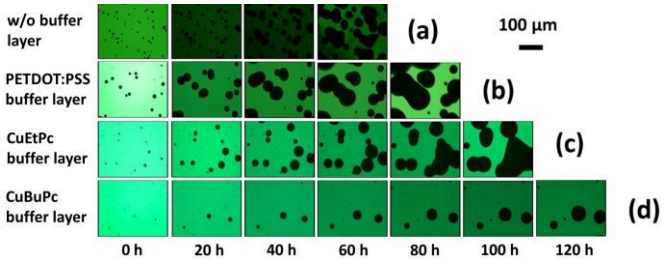

Fig. 6 Micrographs of OLEDs taken after 0, 20, 40, 60, 80, 100 and 120 h of operation at 100 mA/cm^2 under ambient conditions. (a) Type I, (b) Type II, (c) Type III, and (d) Type IV OLEDs.

The quality of the anodic buffer layers should be another factor influencing OLED durability under continuous operation. All the anodic buffer layers possessed smooth surfaces compared with that of the pristine ITO-coated glass substrate (Fig. 2) because the mixture of isomers in the CuPcs decreased the crystallization of the buffer layer, which effectively decreased the pin-hole effect at the interface between the ITO and buffer layers.[20] However, as evidenced by the observation of the growth of dark spots in the OLEDs during operation (Fig. 6), the chemical reaction of PEDOT:PSS with ITO led to instability at the ITO/PEDOT:PSS interface, which typically accelerates OLED degradation.[3,13,16,17] Moreover, the degradation became more serious when the device was exposed to moisture because of the diffusion of a large amount of indium into the polymer layer,[13] promoting the degradation of the polymer and neighboring layers. It has been reported that the ITO surface can react with water to liberate hydroxide and indium that can further diffuse into the emitting layer.[13,47] Because the PEDOT:PSS layer was spin-coated from a water suspension onto an ITO substrate, such a reaction can occur in the ITO/PEDOT:PSS system both during device fabrication and operation in air.[13] Unlike PEDOT:PSS, the preparation of **CuEtPc** and **CuBuPc** thin films from organic solvent and the resulting water-insoluble thin film can markedly suppress the above damage to OLEDs. The enhanced stability of the OLEDs containing these layers is evidenced by the stability of the device operating voltage following ITO surface treatment with **CuEtPc** and **CuBuPc** (Fig. 5b). Indeed, the chemical stability of these Pc materials led to the effective protection of the ITO anode and thus increased OLED durability.

Conclusions

We used two soluble tetraalkyl-substituted CuPcs as anodic buffer layers in OLEDs. The hole-blocking characteristics of these Pc layers markedly slowed hole injection into the Alq_3 emitting layer and thus decreased the production of unstable cationic Alq_3 species, resulting in enhanced OLED efficiency and stability compared with that of devices containing the widely used PEDOT:PSS. The insolubility of the CuPcs in water combined with their extremely high thermal and chemical stability effectively prevented etching of

the ITO anode. This increased the operational stability of the OLEDs in air, which led to the enhancement of OLED durability. These CuPc thin films open a new door to improve the performance of OLEDs containing anode buffer layers.

Acknowledgements

This work was financially supported by the Natural Science for Youth Foundation (Project no. 21303081), Shenzhen Overseas High-level Talents Innovation Plan of Technical Innovation (project no. KQCX20130628152708144), and Special Funds for the Development of Strategic Emerging Industries in Shenzhen (JCYJ20150630145302239).

Notes and references

1 M. P. de Jong, L. J. van IJzendoorn and M. J. A. de Voigt, *Appl. Phys. Lett.*, 2000, **77**, 2255-2257.
2 Y. Lim, Y.-S. Park, Y. Kang, D. Y. Jang, J. H. Kim, J.-J. Kim, A. Sellinger and D. Y. Yoon, *J. Am. Chem. Soc.*, 2011, **133**, 1375-1382.
3 K. R. Choudhury, J. Lee, N. Chopra, A. Gupta, X. Jiang, F. Amy and F. So, *Adv. Funct. Mater.*, 2009, **19**, 491-496.
4 J.-H. Jou, S. Kumar, A. Agrawal, T.-H. Li and S. Sahoo, *J. Mater. Chem. C*, 2015, **3**, 2974-3002.
5 S. A. Carter, M. Angelopoulos, S. Karg, P. J. Brock and J. C. Scott, *Appl. Phys. Lett.*, 1997, **70**, 2067-2069.
6 Y.-J. Choi, S. C. Gong, K.-M. Kang and H-H. Park, *J. Mater. Chem. C*, 2014, **2**, 8344-8349.
7 L. S. Roman, W. Mammo, L. A. A. Pettersson, M. R. Andersson and O. Inganäs, *Adv. Mater.*, 1998, **10**, 774-777.
8 C. Song, Z. Zhong, Z. Hu, J. Wang, L. Wang, L. Ying, J. Wang and Y. Cao, *Org. Electron.*, 2016, **28**, 252-256.
9 X. Wu, J. Liu and G. He, *Org. Electron.*, 2015, **22**, 160-165.
10 J. H. Cook, H. A. Al-Attar and A. P. Monkman, *Org. Electron.*, 2014, **15**, 245-250.
11 H. Choi, B. Kim, M. J. Ko, D.-K. Lee, H. Kim, S.H. Kim and K. Kim, *Org. Electron.*, 2012, **13**, 959-968.
12 K. W. Wong, H. L. Yip, Y. Luo, K. Y. Wong, W. M. Lau, K. H. Low, H. F. Chow, Z. Q. Gao, W. L. Yeung and C. C. Chang, *Appl. Phys. Lett.*, 2002, **80**, 2788-2790.
13 T. P. Nguyen and S. A. de Vos, *Appl. Surf. Sci.*, 2004, **221**, 330-339.
14 J.-S. Kim, P. K. H. Ho, C. E. Murphy, A. J. A. B. Seeley, I. Grizzi, J. H. Burroughes and R. H. Friend, *Chem. Phys. Lett.*, 2004, **386**, 2-7.
15 J.-S. Kim, R. H. Friend, I. Grizzi and J. H. Burroughes, *Appl. Phys. Lett.*, 2005, **87**, 023506.
16 S. A. Choulis, V.-E. Choong, M. K. Mathai and F. So, *Appl. Phys. Lett.*, 2005, **87**, 113503.
17 F. So and D. Kondakov, *Adv. Mater.*, 2010, **22**, 3762-3777.
18 Z. He, H. Wu and Y. Cao, *Adv. Mater.*, 2014, **26**, 1006-1024.
19 T. Mori, T. Mitsuoka, M. Ishii, H. Fujikawa and Y. Taga, *Appl. Phys. Lett.*, 2002, **80**, 3895-3897.
20 Y.-L. Wang, J.-J. Xu, Y.-W. Lin, Q. Chen, H.-Q. Shan, Y. Yan, V. A. L. Roy and Z.-X. Xu, *AIP Adv.*, 2015, **5**, 107205.
21 S. A. Van Slyke, C. H. Chen and C. W. Tang, *Appl. Phys. Lett.*, 1996, **69**, 2160-2162.
22 H. Lee, J. Lee, Y. Yi, S.W. Cho and J. W. Kim, *J. Appl. Phys.*, 2015, **117**, 035503.
23 H. Lee, J. Lee, K. Jeong, Y. Yi, J. H. Lee, J. W. Kim and S. W. Cho, *J. Phys. Chem. C*, 2012, **116**, 13210-13216.
24 R. Bechara, J. Petersen, V. Gernigon, P. Lévêque, T. Heiser, V. Toniazzo, D. Ruch and M. Michel, *Sol. Energy Mater. Sol. Cells*, 2012, **98**, 482-485.
25 M. Raïssi, L. Vignau, B. Ratier, *Org. Electron.*, 2014, **15**, 913-919.
26 J. Meyer, S. Hamwi, T. Bülow, H.-H. Johannes, T. Riedl and W. Kowalsky, *Appl. Phys. Lett.*, 2007, **91**, 113506.
27 H. You, Y. Dai, Z. Zhang and D. Ma, *J. Appl. Phys.*, 2007, **101**, 026105.
28 Y. L. Deng, Y. M. Xie, L. Zhang, Z. K. Wang and L. S. Liao, *J. Mater. Chem. C*, 2015, **3**, 6218-6223.
29 J. L., F. S. Zu, L. Ding, M. F. Xu, X. B. Shi, Z. K. Wang and L. S. Liao, *Appl. Phys. Express*, 2014, **7**, 111601.
30 C. H. Gao, X. Z. Zhu, L. Zhang, D. Y. Zhou, Z. K. Wang and L. S. Liao, *Appl. Phys. Lett.*, 2013, **102**, 153301.
31 Y. H. Lou, M. F. Xu, Z. K. Wang, S. Naka, H. Okada and L. S. Liao, *Appl. Phys. Lett.*, 2013, **102**, 113305.
32 X. L. Zhu, J. X. Sun, H. J. Peng, Z. G. Meng, M. Wong and H. S. Kwok, *Appl. Phys. Lett.*, 2005, **87**, 153508.
33 A. R. Murphy and J. M. J. Fréchet, *Chem. Rev.*, 2007, **107**, 1066-1096.
34 Z. Bao, A. J. Lovinger and A. Dodabalapur, *Appl. Phys. Lett.*, 1996, **69**, 3066-3068.
35 R. Zeis, T. Siegrist and C. Kloc, *Appl. Phys. Lett.*, 2005, **86**, 022103.
36 L. Li, Q. Tang, H. Li, X. Yang, W. Hu, Y. Song, Z. Shuai, W. Xu, Y. Liu and D. Zhu, *Adv. Mater.*, 2007, **19**, 2613-2617.
37 S. Dong, H. Tian, L. Huang, J. Zhang, D. Yan, Y. Geng and F. Wang, *Adv. Mater.*, 2011, **23**, 2850-2854.
38 J. J. Xu, Y. L. Wang, H. Q. Shan, Y. W. Lin, Q. Chen, V. A. L. Roy and Z. X. Xu, Ultrasound-induced Organogel Formation Followed by Thin Film Fabrication via Simple Doctor Blading Technique for Field-Effect Transistor Application, Submitted to ACS Appl. Mater. Interfaces., 2016 (under revision).
39 Y. Inokuma, Z. S. Yoon, D. Kim and A. Osuka, *J. Am. Chem. Soc.*, 2007, **129**, 4747-4761.
40 Z. Deng, Z. Lü, Y. Chen, Y. Yin, Y. Zou, J. Xiao and Y. Wang, *Solid-State Electronics*, 2013, **89**, 22-25.
41 H. Aziz, Z. D. Popovic, N.-X. Hu, A.-M. Hor and G. Xu, *Science*, 1999, **283**, 1900-1902.
42 J. Hwang, H. Kyw Choi, J. Moon, T. Yong Kim, J.-W. Shin, C. Woong Joo, J.-H. Han, D.-H. Cho, J. Woo Huh, S.-Y. Choi, J.-I. Lee and H. Yong Chu, *Appl. Phys. Lett.*, 2012, **100**, 133304.
43 J. Kalinowski, W. Stampor, J. Mężyk, M. Cocchi, D. Virgili, V. Fattori and P. Di Marco, *Phys. Rev. B*, 2002, **66**, 235321.
44 J. Kalinowski, W. Stampor, J. Szmytkowski, D. Virgili, M. Cocchi, V. Fattori and C. Sabatini, *Phys. Rev. B*, 2006, **74**, 085316.
45 J. D. Anderson, E. M. McDonald, P. A. Lee, M. L. Anderson, E. L. Ritchie, H. K. Hall, T. Hopkins, E. A. Mash, J. Wang, A. Padias, S. Thayumanavan, S. Barlow, S. R. Marder, G. E. Jabbour, S. Shaheen, B. Kippelen, N. Peyghambarian, R. M. Wightman and N. R. Armstrong, *J. Am. Chem. Soc.*, 1998, **120**, 9646-9655.
46 H. Vestweber and W. Rieß, *Synth. Met.*, 1997, **91**, 181-185.
47 F. Cacialli, J. S. Kim, T. M. Brown, J. Morgado, M. Granström, R. H. Friend, G. Gigli, R. Cingolani, L. Favaretto, G. Barbarella, R. Daik and W. J. Feast, *Synth. Met.*, 2000, **109**, 7-11.

A table of contents entry

Soluble tetraalkyl-substituted copper phthalocyanines were employed as anodic buffer layers of OLEDs, achieving enhanced stability and durability compared with PEDOT:PSS.